Green Chemistry

PAPER

View Article Online
View Journal | View Issue

Open Access Article. Published on 09 December 2025. Downloaded on 1/24/2026 10:49:46 PM.
This article is licensed under a Creative Commons Attribution 3.0 Unported Licence.

Check for updates

Cite this: *Green Chem.*, 2026, **28**, 839

Life cycle assessment of hydrogen and helium as carrier gases in gas chromatography analysis

Ivan Hetman [a,b]

An attributional life cycle assessment was applied to compare helium and hydrogen as carrier gases for routine gas chromatography. A single functional unit of one chromatographic analysis was used. A ten-year operational period was examined as a utilisation scenario in sensitivity analysis. Three supply routes were modelled: helium obtained as a by-product of natural gas extraction and liquefaction; merchant hydrogen from steam-methane reforming; and on-site hydrogen generation by proton-exchange-membrane electrolysis. System boundaries covered raw material extraction through waste management of laboratory consumables. Capital goods were excluded except for the electrolyser unit. Normalised impact assessment identified marine and freshwater ecotoxicity, human toxicity, climate change, and fossil resource scarcity as dominant categories. On a per-analysis basis, hydrogen performed better than helium in all environmental impact categories due to shorter analysis times and reduced electricity demand, although electrolytic hydrogen showed elevated ecotoxicity from trace-metal emissions in power generation. In the ten-year utilisation scenario, higher chromatographic throughput with hydrogen increased cumulative use of energy and consumables, producing greater total burdens in several midpoint indicators despite superior per-run performance. Uncertainty and sensitivity analyses confirmed the robustness of these results and highlighted electricity sourcing as a critical driver. The main insight is that the comparative advantage of hydrogen arises primarily from reduced analysis time rather than avoidance of helium extraction. Hydrogen is a viable alternative where laboratory safety, mass spectrometry compatibility, and low-carbon electricity are assured. Further reductions require improved consumable management and broader decarbonisation of power supply.

Received 5th November 2025,
Accepted 8th December 2025

DOI: 10.1039/d5gc05912g

rsc.li/greenchem

Green foundation

1. This work advances green analytical chemistry by coupling life cycle assessment with gas chromatographic method design, showing how carrier-gas choice, run time and electricity mix jointly determine environmental performance of routine analyses.
2. Per analysis, hydrogen (on-site electrolysis or steam-methane reforming) lowers impacts across climate change, fossil resource scarcity and human/ecotoxicity because shorter methods reduce electricity demand; electrolytic hydrogen shows higher ecotoxicity where power generation is metal-intensive. Findings are supported by uncertainty and grid-mix sensitivity analyses.
3. Greener outcomes could be achieved by translating these findings into decision-support tools for laboratories, incorporating user-defined electricity mixes, method parameters and consumable policies, and by validating the model across diverse regulatory and industrial settings to identify robust low-impact carrier-gas strategies.

1. Introduction

Gas chromatography (GC) is a widely applied analytical technique for the separation, identification, and quantification of volatile and semi-volatile compounds. Since its introduction in the mid-20th century,[1] GC has become indispensable in pharmaceuticals,[2] environmental,[3] food and beverage,[4] petrochemical,[5] and clinical,[6] analyses. Its broad utility derives from high separation efficiency, sensitivity, and rapid analysis.[7] GC relies on differential partitioning of analytes between a gaseous mobile phase and a stationary column phase.[8] As the vaporized sample travels through the column, driven by the carrier gas, components interact differently with the stationary phase based on their volatility, polarity, and molecular size, resulting in temporal separation and subsequent detection.[8] Carrier gas selection is therefore central, as it not only transports analytes but also influences resolution, retention times, and throughput.[3,8,9] An effective carrier gas must be chemically inert, highly pure

[a]*Laboratory of Organic Electronics, Department of Science and Technology, Linköping University, SE-601 74 Norrköping, Sweden. E-mail: ivan.hetman@liu.se; Tel: +46101034411*
[b]*Clinical Department of Occupational and Environmental Medicine, Region Östergötland, SE-581 85 Linköping, Sweden*

Open Access Article. Published on 09 December 2025. Downloaded on 1/24/2026 10:49:46 PM.
This article is licensed under a Creative Commons Attribution 3.0 Unported Licence.

(≥99.9995%), and detector-compatible.[9] Physical properties as molecular weight, viscosity and diffusivity govern efficiency through the Van Deemter equation.[10] Hydrogen and helium, with low viscosity and high diffusivity, enable higher flow rates and shorter analyses, while nitrogen requires slower velocities and longer run times.[11–13] Thus, gas selection balances analytical performance with safety, cost, and availability.

Helium has long been the preferred carrier gas in capillary GC, offering a combination of analytical and practical benefits.[11,14,15] Its chemical inertness and low molecular weight provide excellent separation efficiency and resolution at higher linear velocities, enabling faster analyses than nitrogen.[12,15] Helium is also non-flammable supporting a safer laboratory environment than hydrogen,[14,16] and is highly compatible with gas chromatography-mass spectrometry (GC-MS) due to its low background and favourable pumping properties, enhancing sensitivity and spectral quality.

Despite its analytical merits, helium poses serious challenges for sustainable laboratory practice, driving the search for alternatives.[17,18] Helium is a finite, non-renewable resource, formed by radioactive decay underground and obtained as a byproduct of natural gas extraction.[18–20] Increasing demand across sectors and limited natural reserves have led to recurring shortages, dramatic price surges, prices quadrupled from 2011 to 2013 and even laboratory shutdowns.[17] The situation is aggravated by geopolitical events, such as the 2017 Qatar blockade, which abruptly removed 30% of global supply.[17,18,21] Market inflexibility and the shift toward unconventional gas sources like shale and biogas with low helium content exacerbate scarcity, while the lack of long-term storage renders supply vulnerable to shocks.[18,19,22] Environmentally, as a byproduct of fossil fuel extraction, helium production is inherently linked to carbon-intensive processes.[20,23] Moreover, once released to the atmosphere, helium escapes to space and is permanently lost from Earth's inventory, making it truly non-renewable.[24]

Hydrogen has emerged as the most promising alternative to helium offering both analytical and sustainability advantages.[11,25] Chromatographically, hydrogen's low viscosity and high diffusivity yield the flattest van Deemter curve and optimal linear velocity (40–60 cm s^{-1}), enabling 1.5–2 times faster analyses than helium without sacrificing separation quality.[11] These properties allow high efficiency across a broad range of conditions and can reduce energy consumption by enabling lower column temperatures.[2,11] Recent studies confirm that method translation from helium to hydrogen is feasible with minimal performance loss, maintaining sensitivity and resolution.[26–28] Crucially, the environmental profile of hydrogen depends strongly on its production route: although hydrogen is often promoted as a sustainable alternative, 96% of global production still relies on fossil energy, with steam methane reforming (SMR) accounting for 80% and producing substantial greenhouse gas emissions.[29] Economically, on-site hydrogen generation *via* electrolysis offers cost and supply advantages.[30–32] However, hydrogen's flammability (explosive at 4–75% in air) requires careful safety management.[33] Modern GC practice addresses these risks with on-site generators (minimal volumes, low pressure), advanced leak detection, automatic shutdown, and robust training, enabling safe laboratory use when protocols are rigorously followed.[33]

Despite increasing efforts to advance sustainable analytical chemistry and substitute helium with hydrogen in GC, a comprehensive life cycle assessment (LCA) directly comparing these carrier gases remains lacking in the peer-reviewed literature. Existing studies have primarily focused on the chromatographic performance and safety aspects of hydrogen substitution.[28,34] However, the environmental burdens across the complete life cycles of helium and hydrogen in GC applications have not been quantified. Such a quantitative LCA is vital for informed laboratory management and evidence-based sustainability decisions.

This study conducts a cradle-to-grave LCA of helium *versus* SMR and water-electrolysed hydrogen in a representative GC workflow, covering gas production, transport or on-site generation, instrument operation, and waste management. Carbon emissions, energy use, resource depletion, and ecotoxicity were assessed; consequently, the first evidence-based comparison of these carrier gases is provided to guide sustainable analytical practice as laboratories face helium shortages and consider hydrogen alternatives.

2. Materials and methods

2.1 Goal and scope

The primary goal of this LCA is to quantitatively compare the environmental impacts associated with the use of helium and hydrogen as carrier gases in routine GC-MS analysis under standard laboratory conditions. The study aims to provide evidence-based guidance for laboratories considering a transition from helium to hydrogen, addressing both technical and sustainability perspectives.

The scope encompasses all relevant life cycle stages from resource extraction or production of each gas, through international and domestic transport, laboratory operation including energy use and consumables to waste treatment and final disposal. Processes that are identical in all scenarios, such as GC-MS instrumentation and analytical columns, are excluded from the comparative boundary to isolate the impact of carrier gas selection. Geographical coverage reflects laboratory operation in Sweden with global sourcing of gases.

This study utilized the U.S. Environmental Protection Agency (EPA) Method 8270E as a representative model for GC-MS analysis of semi volatile organic compounds in environmental matrices.[35] This method is widely recognized for its applicability across various sample types, including water, soil, and solid waste, and is frequently employed in environmental monitoring and regulatory contexts. More details about GC method are available in section 2.3.4 and the SI Table A1.

Open Access Article. Published on 09 December 2025. Downloaded on 1/24/2026 10:49:46 PM.
This article is licensed under a Creative Commons Attribution 3.0 Unported Licence.

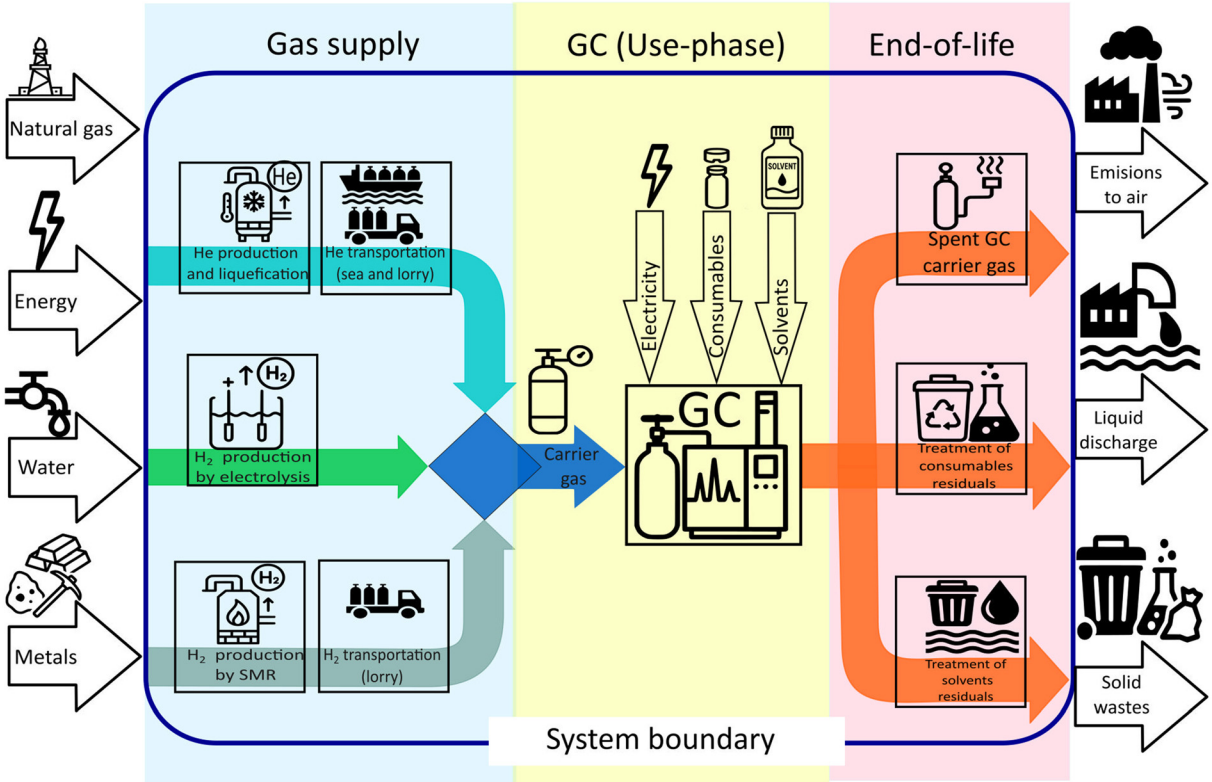

Fig. 1 Material flow and system boundaries.

2.2 Functional unit and system boundaries

The functional unit (FU) was defined as single chromatographic analysis performed under U.S. EPA Method 8270E conditions using a GC-2010Plus (Shimadzu, Japan) with a 30 m × 0.25 mm × 0.25 μm capillary column.

System boundaries include all life cycle stages from raw material extraction to waste treatment, see Fig. 1. For helium, this covers extraction from natural gas, purification, liquefaction, shipping, road transport, laboratory storage, and venting. Hydrogen scenarios model either on-site proton exchange membrane (PEM) electrolysis using grid electricity and deionised water (including ion-exchange resins and desiccants) or SMR with road transport from central Europe. Laboratory operations comprise carrier gas delivery, GC oven, MS detector, vacuum pump energy, and consumables. Downstream processes include gas release, solvent disposal, and recycling of glass, aluminium and polytetrafluoroethylene (PTFE). Infrastructure related to natural gas fields, gas plants, electrolyser or instrument manufacturing, and laboratory buildings is excluded. The study reflects Swedish laboratory practice, regional supply chains, and energy mixes for 2020–2025.

2.3 Life cycle assessment scenarios and life-cycle inventory

This study evaluated three main scenarios for GC-MS carrier gas supply: (1) helium produced as a by-product of natural gas extraction, purified, liquefied, shipped trans-Atlantic, and distributed by road to the laboratory; (2) hydrogen produced *via* SMR at central European facilities, compressed, and transported by road; and (3) hydrogen generated on-site using PEM electrolysis powered by the Swedish electricity grid and deionised water. The scenarios also account for differences in laboratory throughput, method runtimes, and consumable use.

The life-cycle inventory (LCI) for this study was compiled following ISO 14040/44 standards[36,37] and relied on a hybrid approach combining laboratory data, manufacturer specifications, and background datasets from the ecoinvent v3.10 database.[38] Foreground system boundaries included all flows specific to carrier gas production and delivery (helium and hydrogen), instrument energy use, consumables, and waste management associated with GC-MS analysis under U.S. EPA Method 8270E conditions.[35]

Background data for all material and energy flows were sourced from ecoinvent v3.10, ensuring consistency and transparency across scenarios. Laboratory operation parameters including carrier gas flow rates, method run times, and instrument power demand were based on experimental measurements and vendor documentation. All auxiliary flows, such as deionized water, consumables turnover, and hazardous waste management, were accounted for using representative ecoinvent processes. Regional context was set to Sweden, using the Swedish low-voltage electricity mix to capture local grid emissions, "Market for electricity, low voltage, SE". Detailed process inventories and all modelling assumptions are provided in the SI (Tables A1–A11).

Open Access Article. Published on 09 December 2025. Downloaded on 1/24/2026 10:49:46 PM. This article is licensed under a Creative Commons Attribution 3.0 Unported Licence.

2.3.1 Helium production and transportation. Helium supplied to European laboratories is sourced primarily from the Hugoton–Panhandle basin (USA), Ras Laffan (Qatar), Hassi R'Mel (Algeria), and Eastern Siberia (Russia).[39,40] In all cases, helium is produced as a by-product of natural gas extraction, separated *via* cryogenic distillation or pressure-swing adsorption, and subsequently liquefied at approximately 4 K for bulk transport. Liquefied helium is transferred into UN Portable T75 ISO tanks,[41] each with a typical payload of 18 t, and shipped to north-Western Europe, predominantly *via* maritime routes from Houston to Rotterdam (*ca.* 11 000 km). Road transport by EURO 6 lorries then conveys helium to Sweden (1300–1400 km plus 100–500 km regional distribution).

For LCI modelling, the supply chain was parameterized using processes: "Market for helium, liquid, RER" (including natural gas extraction, cryogenic separation, and liquefaction); "Transport, freight, sea, transoceanic ship, GLO" and "Transport, freight, lorry >32 t/16–32 t, EURO6, RER" for inland distribution. Full logistics details are provided in SI Table A4.

2.3.2 On-site hydrogen production by electrolysis. On-site hydrogen for GC was modelled as being produced *via* PEM electrolysis, the preferred technology for analytical laboratories due to its high purity, compact footprint, and rapid start-up.[42,43] PEM electrolysers employ a perfluorosulphonic acid membrane (typically Nafion™), which conducts protons while excluding electrons and gases.[44] Feedwater is oxidized at the anode to generate protons, which traverse the PEM and are reduced to molecular hydrogen at the cathode.[44] Laboratory PEM units routinely deliver hydrogen exceeding 99.999% purity, negating the need for post-purification.[27] Operational modelling employed Swedish low-voltage grid electricity ("Market for electricity, low voltage, SE). Oxygen co-production was accounted for (7.94 kg O_2 per kg H_2) but excluded from the base-case allocation, consistent with typical laboratory venting practice.

The electrolyser stack's cradle-to-gate inventory was adapted from Bareiß *et al.*[45] who provide a detailed bill of materials for a 1 MW industrial stack. For a typical 150 W laboratory-scale electrolyser, material requirements were downscaled using a power-law relationship:

$$M_{\text{scaled}} = M_{\text{ref}} \times \left(\frac{P_{\text{scaled}}}{P_{\text{ref}}}\right)^{\alpha} \quad (1)$$

where P_{ref} = 1000 kW, P_{scaled} = 0.15 kW, and the scaling exponent α = 0.8 to reflect economies of scale.[46] This approach yields 0.087% of the 1 MW stack's material inventory per laboratory unit. See SI Table A5 for details of 0.15 kW laboratory scale stack and processes used for modelling.

Nafion™ is a perfluorinated sulfonic acid polymer based on a tetrafluoroethylene backbone with pendant sulfonic acid groups introduced *via* a proprietary sulfonation process. Due to the lack of direct inventory data for Nafion™ membranes in ecoinvent v3.10, production was modelled using a proxy-based approach as recommended for proprietary or data-deficient processes.[47,48] The backbone was represented by "Market for tetrafluoroethylene, GLO" and membrane fabrication by "Laminating service, foil, with acrylic binder, RER". Sulfonation was approximated by adding "Market for sulfuric acid, RER". All modelling assumptions are presented in SI Table A6.

2.3.3 SMR hydrogen production and transportation. For comparative assessment, hydrogen produced *via* SMR, the predominant industrial method globally and in Europe, was modelled alongside on-site electrolysis. SMR involves reacting natural gas-derived methane with steam, followed by water–gas shift conversion and purification to produce hydrogen.[49] The life cycle system boundaries encompass (i) natural gas extraction and transmission to the reformer, (ii) SMR and water–gas shift conversion, (iii) hydrogen compression to 200–300 bar for road shipment, and (iv) distribution to Swedish laboratories. Inventory modelling utilised the process "Market for hydrogen, gaseous, medium pressure, merchant". Hydrogen is assumed to be distributed *via* road in high-pressure cylinders or tube trailers, with long-haul distances from central European producers (Germany or Netherlands) to southern Sweden, and local distribution. Road transport is represented by "Transport, freight, lorry >32 t/16–32 t, EURO6, RER". See SI Table A8 for details.

2.3.4 GC analysis. The LCA of GC-MS analyses was based on the configuration and operation described in U.S. EPA Method 8270E,[35] employing a Shimadzu GC-2010Plus system with a 30 m × 0.25 mm × 0.25 μm capillary column. Carrier gases, helium and hydrogen, were supplied at ≥99.999% purity and measured flow rates of 13.2 mL min^{-1} for helium (22 min runtime) and 16.2 mL min^{-1} for hydrogen (13.2 min runtime). To ensure comparability, all non-variable components (*e.g.*, columns, hardware) were excluded from the system boundary, focusing the analysis on carrier gas supply, laboratory consumables, instrument energy demand, and waste treatment.

Instrument power requirements included 1.8 kW (GC oven), 1.0 kW (MS detector), and 0.16 kW (vacuum pump), yielding a total 2.96 kW load. Therefore, the helium method consumed 1.09 kWh, while hydrogen required 0.65 kWh per run.

Carrier gas consumption per run was 0.052 g for helium and 0.044 g for hydrogen, calculated using standard densities at 298 K and 1 atm. Sample preparation solvents were inventoried as 2 mL dichloromethane per run ("Market for dichloromethane, RER"). Consumables included a 2.5 g borosilicate autosampler vial ("Market for glass tube, borosilicate, GLO"), a 0.14 g aluminium cap ("Market for aluminium, primary, liquid, GLO"), and a septum comprising 0.14 g synthetic rubber ("Market for synthetic rubber, GLO") and 0.01 g PTFE ("Market for tetrafluoroethylene, GLO"). Detailed life cycle inventories are provided in the SI (see SI Tables A2, A3, A9 and A10).

2.3.5 End-of-life. End-of-life treatment was modelled to reflect standard laboratory waste management practices in Europe. Spent solvents and residual samples were allocated to "Market for hazardous waste, for incineration, Europe without Switzerland", capturing emissions from thermal treatment of chemical waste. Discarded borosilicate vials were primarily routed to "Market for waste glass, SE" to reflect high recycling

Open Access Article. Published on 09 December 2025. Downloaded on 1/24/2026 10:49:46 PM.
This article is licensed under a Creative Commons Attribution 3.0 Unported Licence.

rates in Sweden. Aluminium crimp caps were modelled with "Market for scrap aluminium, Europe without Switzerland", while all PTFE-lined septa entered the municipal solid waste stream, treated as "Market for residues, MSWI, waste rubber, unspecified, Europe without Switzerland". Carrier gases were assumed to be vented at the point of use: helium as inert loss to atmosphere, and hydrogen as rapid oxidation to water vapour. These pathways reflect standard laboratory ventilation and waste gas protocols. All background data and process selections are documented in the SI (SI Tables A2 and A3).

2.4 Impact assessment

Environmental impacts were evaluated using six categories from the ReCiPe 2016 Midpoint (H) method: Global Warming Potential (GWP), Fossil Resource Scarcity (FRS), Freshwater Ecotoxicity (FWE), Marine Ecotoxicity (ME), Human Carcinogenic Toxicity (HCT), and Human Non-carcinogenic Toxicity (HnCT). For more details on selecting these categories, see section 3.1. All impact assessments were conducted in OpenLCA software (GreenDelta, Germany) using ecoinvent v3.10 datasets with the APOS system model and process-based allocation. Impact category selection reflects international best practice (ISO 14040/44)[36,37] and relevance for analytical laboratories. Results were normalized to global annual impact levels using the ReCiPe 2016 World (2010) H normalization factors, enabling direct comparison across impact categories and scenarios.

2.5 Sensitivity and uncertainty analysis

To assess the robustness of the LCA results, a comprehensive sensitivity analysis was conducted on key foreground parameters influencing the environmental performance of workflows. Scenarios explored included variations in electricity supply (Sweden, EU-27, USA, China, Brazil, and 100% photovoltaic), reflecting differences in carbon intensity and grid mix. Additional analyses evaluated the impact of alternative hydrogen production routes (on-site electrolysis *vs.* SMR).

Laboratory scheduling scenarios were also tested, comparing standard *versus* continuous operation and associated throughput. It was additionally evaluated GC operation under typical laboratory scheduling over a 10 year horizon, corresponding to 2000 hours per year (8 h per day, 5 days per week, 50 weeks per year). Total analyses equate to about 54 500 with helium and 90 900 with hydrogen, reflecting higher throughput enabled by hydrogen's shorter method runtime. This utilisation test is treated as a scenario, distinct from the service-based functional unit, to avoid conflating efficiency (per analysis) with cumulative output.

To examine modelling-approach sensitivity, the life cycle impact assessment (LCIA) for a single analysis was calculated under both attributional and consequential system models, holding the foreground and impact method constant. Results were compared to isolate the effect of average *versus* marginal background linkages and substitution rules.

Parameter uncertainty in this LCA was addressed using Monte Carlo simulation and scenario analysis. Key sources of uncertainty included instrument power demand, carrier gas flow rates, laboratory conditions (temperature, pressure), and operational factors such as instrument idle periods and method variations. Further uncertainty arises from batch variability in consumables, solvent purity, and differences in laboratory protocols.

To systematically capture these uncertainties, input flows including carrier gases, solvents, consumables, and lorry transportation were assigned lognormal distributions with a geometric standard deviation (GSD) of 1.2, reflecting moderate operational and production variability. Electricity consumption was modelled with a lognormal distribution and a GSD of 1.1, justified by its more precise measurement and lower variability. The number of analyses performed over the study period was similarly treated as lognormal (GSD 1.2), capturing operational uncertainties such as downtime and maintenance. For sea freight of helium, a uniform distribution was used between 11 280 km and 21 000 km, representing plausible minimum and maximum shipping distances based on global supply routes. End-of-life flows were assigned lognormal distributions with GSD 1.2, mirroring the input material uncertainties. This consistent approach ensures that uncertainty is propagated realistically across all stages of the carrier gas life cycles.

3. Results and discussion

3.1 Selection of priority impact categories based on normalised LCIA results

The identification of priority LCIA categories in this study was guided by normalized impact scores (see Fig. 2 and SI Table A11), which enable direct comparison across categories of differing units and magnitudes.

Normalization revealed that four midpoint indicators ME, FWE, HCT, HnCT were consistently at least one order of magnitude higher than all other categories for every carrier gas scenario. As a result, these impact categories were selected for detailed analysis, following established LCA practice to focus interpretation on those endpoints with the greatest normalized or policy-relevant scores.[50,51] While GWP is typically a central metric in environmental LCA, its normalized score in this study (*e.g.*, 1.10×10^{-5} for GC He) was lower than those of the toxicity-related categories. Nonetheless, climate change GWP remains an essential category for international benchmarking and for comparability with earlier LCA studies. FRS also emerges as a priority due to the fossil-based origin of He and, in the SMR H_2 scenario, underscoring concerns about the long-term sustainability of laboratory gas supply chains.[52]

3.2 Marine ecotoxicity and freshwater ecotoxicity

FWE and ME were identified as the most responsive midpoint indicators in normalised life-cycle screening. Disaggregating the inventory into five foreground modules: electricity, chemicals and consumables, carrier-gas supply, transport and end-of-life, shows a remarkably uniform picture (Fig. 3 and SI

Open Access Article. Published on 09 December 2025. Downloaded on 1/24/2026 10:49:46 PM.
This article is licensed under a Creative Commons Attribution 3.0 Unported Licence.

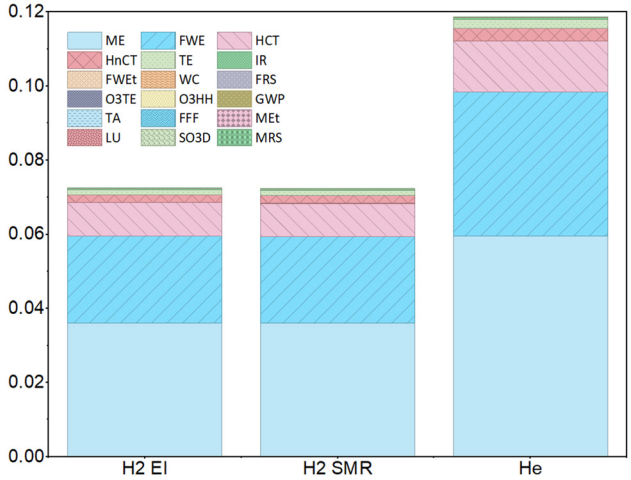

Fig. 2 Life cycle impact assessment results normalisation. Impact categories: ME – marine ecotoxicity; FWE – freshwater ecotoxicity; HCT – human carcinogenic toxicity; HnCT – human non-carcinogenic toxicity; TE – terrestrial ecotoxicity; IR – ionizing radiation; FWEt – freshwater eutrophication; WC – Water consumption; FRS – fossil resource scarcity; O3TE – ozone formation, terrestrial ecosystems; O3HH – ozone formation, human health; GWP – global warming potential; TA – terrestrial acidification; FFF – fine particulate matter formation; MEt – marine eutrophication; LU – land use; SO3D – stratospheric ozone depletion; MRS – mineral resource scarcity.

Table A12). Irrespective of whether the carrier gas is helium, electrolytic or SMR hydrogen low-voltage electricity drawn by the GC oven, MS detector and vacuum pump dominates the aquatic burden, supplying about 97% of FWE and about 96% of ME per chromatogram.

Per-run impacts follow the rank order H_2 electrolysis ≈ H_2-SMR < He. FWE is 2.88×10^{-2}, 2.87×10^{-2} and 4.76×10^{-2} kg 1,4-DCB-eq. (1,4-dichlorobenzene equivalents) for the three routes; ME is 3.73×10^{-2}, 3.72×10^{-2} and 6.15×10^{-2} kg 1,4-DCB-eq., respectively. The helium penalty stems almost entirely from the longer 22 min oven programme (*versus* 13 min for hydrogen), which increases electricity demand by 59%. The electricity itself is responsible for ecotoxicity because of trace metals embedded in the Swedish grid mix: copper in conductors, zinc galvanisation, nickel–chromium steel alloys in hydro-dam components. In the ecoinvent datasets these metals appear as dissolved ions or particulates released during mining, smelting and slag disposal. Direct gas streams are essentially irrelevant ($\leq 3 \times 10^{-5}$ kg 1,4-DCB-eq.) because helium and hydrogen are non-toxic and employed at millilitre-per-minute flow rates.

3.3 Human toxicity (carcinogenic and non-carcinogenic)

HCT and HnCT potentials are the second-largest contributors to the life-cycle profile of GC analysis, superseded only by aquatic ecotoxicity. Per-run results span 0.024–0.038 kg 1,4-DCB-eq. for HCT and 0.314–0.512 kg 1,4-DCB-eq. for HnCT (lowest for hydrogen produced by electrolysis, highest for helium). Across all scenarios electricity generation is the dominant hotspot, supplying 79–87% of HCT and 93–95% of HnCT. Inventory inspection links these burdens principally to trace-metal releases from power production: Cr(VI) from and stainless-steel manufacture shapes the carcinogenic score, while Zn, As and Pb emitted during base-metal mining, smelting and ash disposal drive HnCT. Helium carries a higher electricity share per analysis (0.033 kg 1,4-DCB-eq.) than either electrolytic or SMR hydrogen (≈0.020 kg 1,4-DCB-eq.) because its 22 min temperature programme consumes 59% more power than the 13.2 min hydrogen method.

Chemicals and consumables as borosilicate vials, aluminium caps, PTFE–silicone septa and solvents add a further about 15% to HCT and about 4% to HnCT. These impacts originate from Cr(VI) and organochlorine releases during glass melting and chlor-alkali processing. End-of-life incineration of waste solvent and polymer raises both human toxicity categories by another 5%, *via* fly-ash metals and dioxin precursors. Carrier gases themselves are essentially benign (<0.3% of either indicator) and transport is negligible (<0.01%) because most upstream energy is embedded in electricity.

3.4 Global-warming potential

GWP is a decisive midpoint indicator for ranking helium against hydrogen carrier options, even though a single GC determination emits only tens of grams of CO_2-equivalent. Across all scenarios electricity is the dominant source of greenhouse-gas (GHG) emissions because it powers the GC oven, MS and vacuum pump, and when hydrogen is produced on-site by PEM electrolysis drives water splitting. Under the Swedish grid mix used as baseline (≈20 g CO_2-eq. per kWh),[53] a single analysis with electrolytic or SRM H_2 causes 0.0596 kg CO_2-eq., whereas the helium method is 46% higher at 0.0876 kg CO_2-eq. Electricity supplies 69–79% of these totals, with CO_2 (>95%) the main contributor and upstream CH_4 leakage from natural-gas fields explaining the marginal gap between electrolysis- and SMR-hydrogen.

Laboratory consumables as borosilicate vials, aluminium caps, PTFE–silicone septa and solvents add a uniform 0.011–0.012 kg CO_2-eq. (≈15% of the H_2 total). Their footprint originates from fuel burnt in glass melting, primary-aluminium electrolysis and petrochemical feedstocks. End-of-life incineration of spent solvents and septa contributes a further 6–7% through direct CO_2 and N_2O emissions. Carrier-gas losses and road transport of cylinders remain negligible (<0.5%). The higher electricity share in the helium scenario reflects the energy-intensive cryogenic separation and −269 °C liquefaction required upstream.

3.5 Fossil resource scarcity

FRS captures the cumulative withdrawal of crude oil, natural gas and coal across the life cycle of a GC determination. Because GC laboratories operate continuously, use disposable petro-based consumables and, in two of the three carrier-gas options, rely on energy-intensive gas production, FRS provides an integrative view of non-renewable resource pressure.

For one analysis electricity is the unequivocal hotspot, supplying 68–76% of total FRS in both hydrogen scenarios

Open Access Article. Published on 09 December 2025. Downloaded on 1/24/2026 10:49:46 PM.
This article is licensed under a Creative Commons Attribution 3.0 Unported Licence.

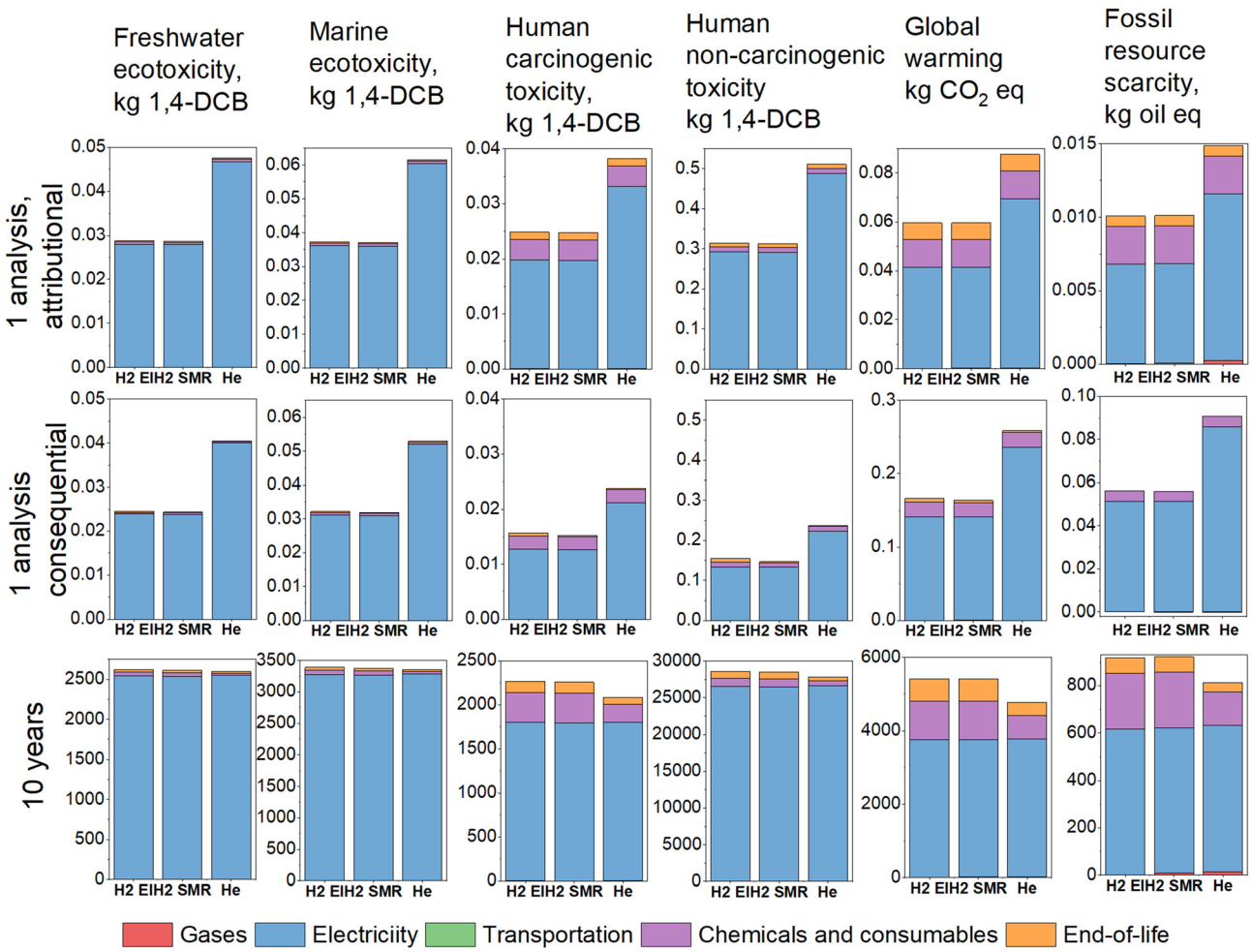

Fig. 3 Life cycle impact assessment.

(0.00675–0.00677 kg oil eq. of 0.0101 kg oil eq.) and 76% in the helium scenario (0.01131 kg oil eq. of 0.01489 kg oil eq.). The higher helium score (+49% relative to electrolytic hydrogen) stems from two factors: (i) a 22 min temperature programme *versus* 13.2 min with hydrogen, which raises instrument power demand, and (ii) the cryogenic separation, liquefaction and boil-off losses required to obtain analytical-grade liquid helium, adding 2.60×10^{-4} kg oil eq. Chemicals and consumables (borosilicate vials, aluminium caps, PTFE/silicone septa and solvents) account for roughly one-quarter of the hydrogen totals but only 17% for helium, reflecting identical per-run masses but higher electricity elsewhere. End-of-life incineration contributes 7% across all cases through the combustion of solvent residues and polymer waste, whereas the gases themselves are almost negligible (<2% for He; <0.3% for H_2). Transport of cylinders and consumables is trivial (<0.05%).

Laboratory electricity is the controlling variable for FRS. Single-use consumables form the second-largest lever, particularly when high sample throughput is sought. Carrier-gas manufacture affects results far less than either electricity or consumables because GC uses only millilitre-per-minute flows, yet differences between helium and hydrogen pathways remain noticeable: cryogenic helium is more fossil-intensive per unit gas, whereas SMR-H_2 incurs additional natural-gas embodied energy. Switching from helium to on-site electrolytic hydrogen reduces per-analysis FRS by half, but its long-term advantage narrows unless concurrent measures electricity demand and consumable turnover.

3.6 Stand-alone impact of carrier-gas supply

Isolating the gas node from the wider foreground inventory clarifies how helium and high-purity hydrogen influence six priority impact categories (see Fig. 4). Per-run results reveal helium as the most resource- and climate-intensive choice, whereas electricity-intensive water electrolysis is most burdensome for toxicity-related endpoints.

Electrolytic hydrogen exhibits the highest ecotoxicity per analysis, with values of 9.8×10^{-5} kg and 1.3×10^{-4} kg 1,4-DCB-eq. for FWT and ME, respectively ten times higher than SMR hydrogen and an order of magnitude greater than helium. More than 90% of these impacts are attributable to copper and zinc emissions from electricity generation signifi-

Open Access Article. Published on 09 December 2025. Downloaded on 1/24/2026 10:49:46 PM.
This article is licensed under a Creative Commons Attribution 3.0 Unported Licence.

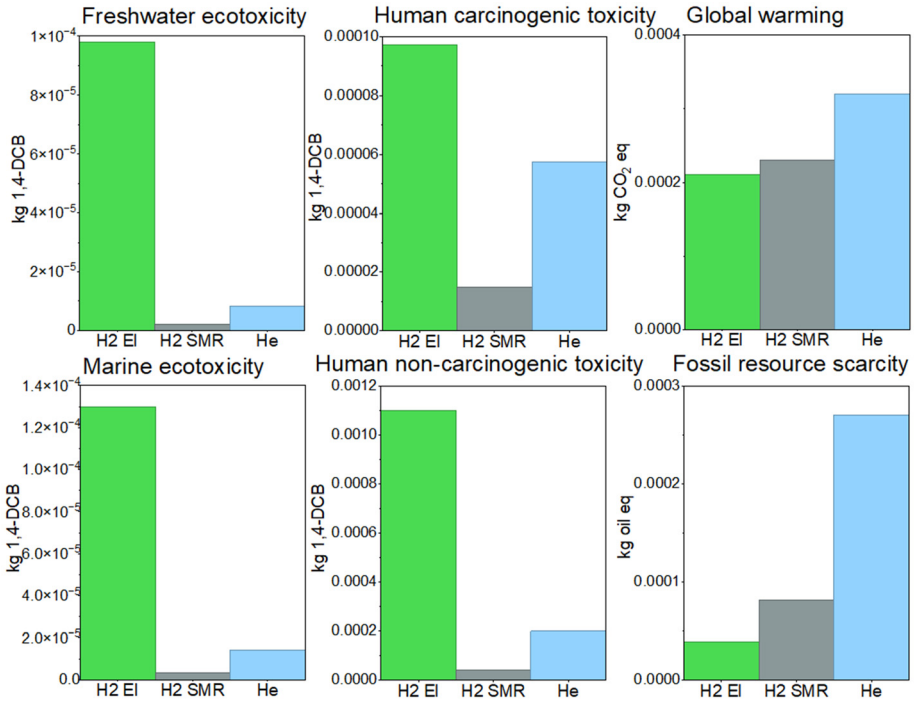

Fig. 4 Stand-alone impact of carrier-gas supply.

cantly increasing the metal-related burden. Electricity also dominates health-related endpoints. Per run, electrolysis-H_2 produces the highest HCT (9.7×10^{-5} kg 1,4-DCB-eq.) and HnCT (1.1×10^{-3} kg 1,4-DCB-eq.) burdens, driven by Cr(VI), Zn, As and Pb emitted in power generation and metal refining.

Helium displays the highest global warming impact per analysis (3.2×10^{-4} kg CO_2-eq.), compared to 2.1×10^{-4} kg for electrolysis-derived hydrogen and 2.3×10^{-4} kg for SMR hydrogen. This elevated footprint is largely due to the electricity required for helium liquefaction, which produces 6.9×10^{-4} kg CO_2-eq. per run, substantially more than is needed for hydrogen compression. The small difference between the two hydrogen scenarios is primarily attributed to methane emissions from natural gas extraction.

For FRS, each helium-based chromatogram requires 2.7×10^{-4} kg oil-eq. which is three times higher than on-site electrolysis hydrogen (3.9×10^{-5} kg oil-eq.) and double that of SMR H_2 (8.2×10^{-5} kg oil-eq.). This difference arises primarily from the substantial natural gas input needed for helium's cryogenic purification and liquefaction. In contrast, Swedish grid electricity used for PEM electrolysis is predominantly non-fossil, minimizing the fossil burden of on-site hydrogen production, indicating helium remains the most fossil-intensive carrier even after normalizing for analytical throughput.

3.7 Sensitivity

Per-run results show consistent advantages for hydrogen across all selected categories, independent of production route (Fig. 2, 3 and SI Tables A11, A12). When scaled to a ten-year operating horizon, the higher throughput enabled by shorter hydrogen methods increases absolute resource use and emissions. This distinction underscores the need to interpret both efficiency (per analysis) and effectiveness (cumulative analytical output over time). To identify drivers, impacts were disaggregated by life-cycle stage, including carrier-gas supply, transport, electricity, consumables, and end-of-life; interpretation follows normalized midpoint indicators as recommended in contemporary LCIA.

At cumulative scale (90 900 GC analysis using hydrogen as the carrier gas *versus* 54 500 helium-based GC runs), electricity remains dominant, see Fig. 3 and SI Table A14. For aquatic toxicity, electricity supplies at least 97% of totals, giving about 2.54×10^3 kg 1,4-DCB-eq. FWE for each hydrogen pathway and 2.59×10^3 kg for helium; ME is within ±2% of these values. Although helium requires fewer runs, longer programs yield nearly the same cumulative electricity demand as faster hydrogen methods, so per-run gains diminish in aggregate.

Non-electrical modules increase modestly with high throughput. Consumables (vials, aluminium caps, PTFE septa, solvents) contribute 1.7–1.8% of aquatic toxicity for hydrogen but 1.0% for helium, reflecting 67% greater solvent and vial use with hydrogen; end-of-life follows the same pattern. These increments remain small relative to electricity.

Human toxicity is similarly electricity-led. Over ten years, electricity accounts for about 80% of HCT (1791–1801 kg 1,4-DCB-eq.) and about 95% of HnCT (26 500–26 700 kg 1,4-DCB-eq.) across scenarios. Cumulative HCT totals 2264 kg (H_2 El), 2256 kg (H_2 SMR), and 2082 kg (He); HnCT totals are 28 600, 28 500, and 27 000 kg 1,4-DCB-eq., respectively. Consumables scale with injections (340 kg and 1110 kg for HCT and HnCT

 This journal is © The Royal Society of Chemistry 2026

Open Access Article. Published on 09 December 2025. Downloaded on 1/24/2026 10:49:46 PM.
This article is licensed under a Creative Commons Attribution 3.0 Unported Licence.

in hydrogen workflows), while end-of-life contributes 124 kg and 918 kg; gas production and transport remain below 0.5%.

For GWP, electricity contributes 82–87% of cumulative impacts, giving 5.42 t CO_2-eq. for both hydrogen pathways and 4.77 t CO_2-eq. for helium. Methane losses raise the H_2 SMR total by about 22 kg CO_2-eq. relative to electrolysis. Consumables contribute 1.05 t CO_2-eq. (H_2) *versus* 0.63 t (He), and end-of-life adds 0.61 t *versus* 0.37 t; transport, including cryogenic helium shipping, remains below 1 t CO_2-eq.

FRS is likewise electricity-dominated: 615–617 kg oil-eq. per scenario (73% of helium's 849 kg oil-eq.; 69–70% of hydrogen's 872–891 kg oil-eq.). Consumables reach 236 kg oil-eq. (H_2) *versus* 141 kg (He); end-of-life is 65–66 kg *versus* 39 kg. Gas production is minor (H_2 El 1.37 kg oil-eq.; H_2 SMR 7.35 kg; He 14.2 kg).

To test the robustness of our baseline results it was recalculated the LCI with six contrasting electricity mixes: hydro- and nuclear-dominated Sweden (reference), the interconnected EU-27 grid, the United States average mix, coal-intensive China, hydropower-rich Brazil and a prospective 100% behind-the-meter photovoltaic (PV) supply. All other foreground processes as gas production routes, consumables, transport distances and waste handling were kept constant. Fig. 5 and SI Table A15 report scores for the five midpoint indicators previously identified as decision-relevant.

Substituting the Swedish grid by the Chinese mix raises the electricity-related CO_2 of the electrolysis scenario from 0.041 to 0.338 kg CO_2-eq., elevating total GWP per one GC run from 0.060 to 0.662 kg CO_2-eq. FRS climbs in parallel (1.0×10^{-2} to 9.4×10^{-2} kg oil-eq.) as coal-mine methane and residual fuel oils dominate Chinese power generation. Heavy metals in coal fly-ash also amplify FWE (0.0288 to 0.0523 kg 1,4-DCB-eq.) and HnCT (0.315 to 0.648 kg 1,4-DCB-eq.). Helium proves even more sensitive: under PV electricity its GWP contracts to 0.106 kg CO_2-eq., whereas under the Chinese grid it reaches 1.10 kg CO_2-eq., twice that of any hydrogen route. Brazil's largely hydroelectric mix yields comparatively low GWP and FRS but triples water consumption per run owing to reservoir evaporation. The PV scenario delivers the lowest GWP and FRS yet increases mineral-resource depletion and ecotoxicity by 20–25%.

Sensitivity to system model was evaluated by recalculating per-run impacts with attributional and consequential LCI while holding the functional unit, process structure, and LCIA method constant, see Fig. 1 and SI Tables A12, A13). In both models, hydrogen retained lower impacts than helium per analysis across the target categories, yet magnitudes and burden shares differed systematically. Electricity remained the dominant contributor but was consistently smaller under consequential modelling. For electrolytic hydrogen, electricity-related FWE declined from 0.02798 to 0.02392 kg 1,4-DCB-eq., and ME from 0.03608 to 0.03109 kg 1,4-DCB-eq. Helium showed similar reductions (electricity: 0.06030 to 0.05196 kg 1,4-DCB-eq. for ME). Human toxicity endpoints exhibited the same pattern: for electrolytic hydrogen, electricity fell from 0.01977 to 0.01264 kg 1,4-DCB-eq. (HCT) and from 0.29224 to 0.13328 kg 1,4-DCB-eq. (HnCT); helium decreased from 0.03304 to 0.02113 and from 0.48848 to 0.22278 kg 1,4-DCB-eq., respectively. These shifts are consistent with the use of marginal suppliers and substitution rules embedded in conse-

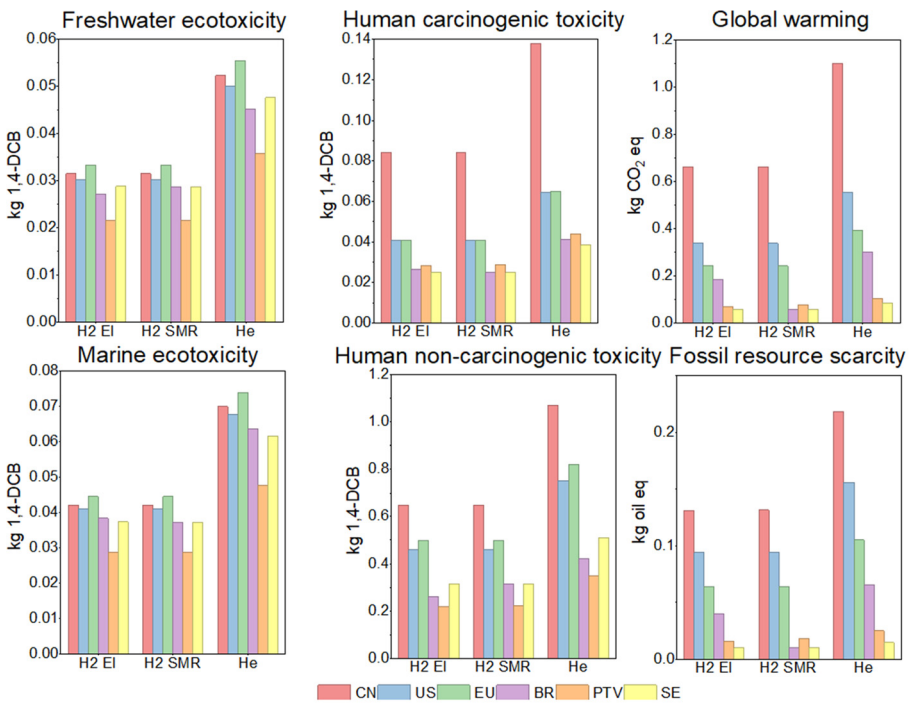

Fig. 5 Life cycle impact sensitivity for different power grids.

Open Access Article. Published on 09 December 2025. Downloaded on 1/24/2026 10:49:46 PM.
This article is licensed under a Creative Commons Attribution 3.0 Unported Licence.

quential system models, which can materially alter electricity's composition relative to average mixes used in attributional modelling.[51,54]

For GWP, electricity again dominated and declined in the consequential results: electrolytic hydrogen fell from 0.29224 to 0.13328 kg CO_2-eq.; SMR hydrogen from 0.29129 to 0.13285 kg CO_2-eq.; helium from 0.48848 to 0.22278 kg CO_2-eq. Small residual differences between hydrogen routes persisted, reflecting methane losses in natural-gas supply to SMR. The sensitivity of toxicity and climate results to electricity is congruent with the literature identifying power generation as a principal driver of LCIA outcomes.[55]

In contrast, FRS rises markedly under consequential modelling owing to the different representation of marginal energy supply: for electrolysis-hydrogen, electricity increases from 0.04131 to 0.14119 kg oil-eq.; for helium, 0.06905 to 0.23599 kg oil-eq. This divergence, lower GWP but higher FRS, highlights that the consequential provider set can embody a distinct primary-energy profile from the attributional average, altering category rankings even when total electricity per run is unchanged. The observation is consistent with the conceptual distinction between attributional (average, share-of-burden) and consequential (decision-induced, marginal) modelling and the possibility that marginal mixes differ materially from averages.

Switching from attributional to consequential modelling compresses electricity-dominated categories at the single-run scale and introduces substitution credits at end-of-life, but it does not alter the core conclusion: hydrogen retains lower per-analysis impacts than helium across all target categories.

3.8 Study uncertainty and limitations

Three main types of uncertainty were identified: parameter, methodological, and scenario uncertainty (ISO 14044).[36] Parameter uncertainty stemmed from variability in electricity consumption, chemical use, and transport distances. The influence of electricity was especially pronounced: grid mix and carbon intensity varied substantially across regions directly impacting results for hydrogen production, see 3.7.

Chemical and consumable inputs (*e.g.*, ion-exchange resins, vials, caps, solvents) also contributed to parameter uncertainty. Although ecoinvent averages were used, real laboratory practices vary, especially regarding solvent consumption, vial reuse, and recycling rates, affecting ecotoxicity and toxicity results.

Methodological uncertainty in this study primarily encompasses: (i) the choice of LCIA method and indicators (ReCiPe 2016 midpoint, selection of priority categories), (ii) the use of midpoint rather than endpoint indicators, (iii) the adoption of an attributional ecoinvent system model (APOS) rather than a consequential model, and (iv) the exclusion of capital goods and infrastructure in line with product-level LCA conventions. These choices can influence absolute impact levels but are unlikely to invert the relative ranking of helium and hydrogen, because electricity and consumables dominate across reasonable methodological variants, as shown by the attributional–consequential and grid-mix sensitivity analyses.

Scenario uncertainty encompassed assumptions about future technology, operational conditions, and supply chains. Helium's environmental profile was especially sensitive to changes in extraction technology, global supply dynamics, and transport logistics. For hydrogen, advances in electrolyser efficiency, membrane durability, and scale could alter environmental impacts over time. Transport scenarios, particularly for helium, added further variability depending on shipping routes and distances.

A comprehensive uncertainty analysis was conducted using Monte Carlo simulations to evaluate the robustness of the LCA results for both single GC analyses and cumulative impacts over a ten-year operational period, see Table 1 and Fig. 6.

The results showed that helium consistently exhibited higher mean impacts and greater variability across all midpoint categories compared to hydrogen, whether produced by electrolysis or SMR. For example, the GWP per helium analysis (mean = 0.088 kg CO_2-eq., SD = 0.007) exceeded that of electrolysis hydrogen (mean = 0.060 kg CO_2-eq., SD = 0.004) and SMR hydrogen (mean = 0.060 kg CO_2-eq., SD = 0.004). The increased

Table 1 Uncertainty of life cycle impact assessment

Impact category, reference unit	Hydrogen, electrolysis		Hydrogen, SMR		Helium	
	SD	Mean	SD	Mean	SD	Mean
ME, kg 1,4-DCB eq.	0.037	0.003	0.037	0.003	0.061	0.006
FWE, kg 1,4-DCB eq.	0.029	0.003	0.029	0.003	0.048	0.005
GWP, kg CO_2 eq.	0.060	0.004	0.060	0.004	0.088	0.007
HCT, kg 1,4-DCB eq.	0.025	0.002	0.025	0.002	0.038	0.003
HnCT, kg 1,4-DCB eq.	0.315	0.028	0.314	0.028	0.511	0.047
FRS, kg oil eq.	0.010	0.001	0.010	0.001	0.015	0.001

SD – standard deviation.

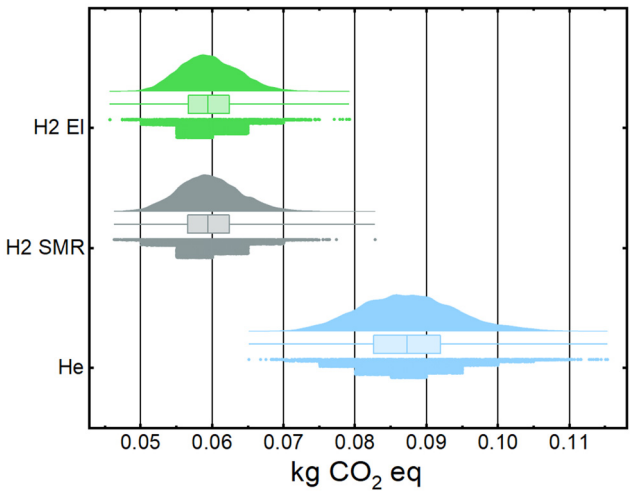

Fig. 6 Uncertainty for GWP impact category.

 This journal is © The Royal Society of Chemistry 2026

Open Access Article. Published on 09 December 2025. Downloaded on 1/24/2026 10:49:46 PM.
This article is licensed under a Creative Commons Attribution 3.0 Unported Licence.

uncertainty for helium primarily arose from the electricity-intensive processes of liquefaction, cryogenic storage, and long-distance transport. Similarly, FRS for helium (mean = 0.015 kg oil-eq., SD = 0.001) reflected the high fossil fuel dependency of its supply chain.

For FWE and ME, electrolysis and SMR H_2 exhibited lower absolute impacts than helium but displayed similar proportional uncertainties (standard deviations of approximately 9–10% of the mean). These uncertainties were mainly driven by trace metal emissions in electricity generation, particularly in grids with significant hydro or coal contributions.

HCT and HnCT also exhibited substantial uncertainty, influenced by emissions of heavy metals from electricity production and consumable manufacturing. For example, mean human HnCT for helium (0.511 kg 1,4-DCB-eq., SD = 0.047) was higher and more variable than for hydrogen scenarios (0.314–0.315 kg 1,4-DCB-eq., SD = 0.028).

This study provides a comprehensive LCA of helium and hydrogen as carrier gases in GC analysis, yet several limitations should be acknowledged. First, the assessment relies on secondary data from ecoinvent and manufacturer specifications, which may not fully capture real-world variations in laboratory practices such as solvent use, consumables management, and instrument maintenance. Second, the system boundaries exclude infrastructure and capital goods such as laboratory buildings, GC-MS instruments and columns from the system boundaries, consistent with product-level attributional LCA practice. Including their environmental burdens would increase absolute impacts for all scenarios but would not directly affect carrier-gas consumption or the relative differences between helium and hydrogen, because identical instrumentation and laboratory context are assumed in each case. This may underrepresent long-term resource and energy demands. Equipment production for large-scale hydrogen and helium generation was also excluded, as appropriate allocation to the fraction used in GC is not feasible; by contrast, the production of local electrolysis units for on-site hydrogen generation was included, as these are directly linked to the laboratory context.

Importantly, several gas properties critical to GC performance were not addressed in the LCA. The safety risks associated with hydrogen's explosiveness, its limitations for GC-MS applications, and the higher noise levels observed with hydrogen, despite its faster analysis times, were not evaluated. The compatibility of hydrogen with future generations of GC-MS equipment remains uncertain and warrants further investigation.

Additionally, the electricity mix and technological assumptions reflect current conditions; future grid decarbonization, unexpected supply fluctuations, or technological advances could alter environmental impacts. While sensitivity analyses explored major sources of uncertainty, impacts from accidental gas releases or laboratory safety incidents were not considered. These limitations identify areas for further research and refinement and underscore the need to integrate technical and safety considerations alongside environmental assessments.

4. Conclusions

This study presents the first comprehensive LCA comparing the environmental impacts of helium and hydrogen as carrier gases in GC workflows, with specific focus on laboratory-scale operations. The results demonstrate that, on a per-analysis basis, hydrogen whether produced by on-site electrolysis or SMR generally outperforms helium in key environmental impact categories, including GWP and FRS. However, hydrogen generated *via* electrolysis incurs higher FWE and ME impacts, largely due to trace metal emissions from electricity production. Over a ten-year operational period, the greater throughput enabled by hydrogen narrows the differences in cumulative impacts, highlighting the importance of considering both analytical efficiency and total environmental footprint.

It is important to emphasize that the observed environmental efficiency of transitioning from helium to hydrogen arises mainly from the shorter analysis time enabled by hydrogen, which substantially reduces electricity consumption per sample. In contrast, factors such as the fossil origin of helium, which are often highlighted contribute relatively little to the overall impact in this laboratory context.

Electricity supply emerges as the dominant contributor to most impact categories, underscoring the crucial role of low-carbon grids in realizing the environmental benefits of hydrogen. The study also highlights the influence of laboratory consumables and operational practices, suggesting that further reductions require not only optimal carrier gas selection, but also efficient laboratory management and sustainable material sourcing.

Overall, these findings support the transition to hydrogen as a more sustainable alternative to helium, provided that safety, compatibility with GC-MS instrumentation, and local energy sourcing are carefully considered. Future research should integrate technical, safety, and economic aspects with environmental assessments to guide sustainable practice in analytical laboratories.

Author contributions

Ivan Hetman: conceptualization, funding acquisition, methodology, investigation, formal analysis, data curation, visualization, writing – original draft, review and editing.

Conflicts of interest

There are no conflicts to declare.

Data availability

All data supporting the findings of this study are provided in the article and its supplementary information (SI). Supplementary information: (i) full foreground life cycle inventories for all scenarios at the per-analysis and ten-year scales (gas supply, electricity, consumables, end-of-life), (ii) detailed

Open Access Article. Published on 09 December 2025. Downloaded on 1/24/2026 10:49:46 PM.
This article is licensed under a Creative Commons Attribution 3.0 Unported Licence.

descriptions of the GC method and operating parameters, (iii) attributional and consequential LCIA results by life-cycle stage for all impact categories, and (iv) grid-mix sensitivity results and normalised scores. Background life cycle data were obtained from the ecoinvent database (version and system model as specified in the Methods section) under a commercial licence and cannot be redistributed; readers with ecoinvent access can reproduce the calculations using the inventories. See DOI: https://doi.org/10.1039/d5gc05912g.

Acknowledgements

This work was supported by the Swedish Foundation for Strategic Research [grant APR23-0012]. The author gratefully acknowledges Harry Tibbetts for his careful reading of the manuscript and for providing constructive comments as the first reader of this work.

References

1 A. T. James and A. J. P. Martin, *Biochem. J.*, 1952, **50**, 679–690, DOI: 10.1042/bj0500679.
2 F. Bernardoni, H. M. Halsey, R. Hartman, T. Nowak and E. L. Regalado, *J. Pharm. Biomed. Anal.*, 2019, **165**, 366–373, DOI: 10.1016/j.jpba.2018.12.006.
3 F. J. Santos and M. T. Galceran, *TrAC, Trends Anal. Chem.*, 2002, **21**, 672–685, DOI: 10.1016/S0165-9936(02)00813-0.
4 B. Lv, W. Mo, C. Jian, S. Li and Y. Guo, *J. Food Meas. Charact.*, 2024, **18**, 8002–8015, DOI: 10.1007/s11694-024-02782-6.
5 J. B. Gilman, B. M. Lerner, W. C. Kuster and J. A. De Gouw, *Environ. Sci. Technol.*, 2013, **47**, 1297–1305, DOI: 10.1021/es304119a.
6 W. Miekisch, J. K. Schubert and G. F. E. Noeldge-Schomburg, *Clin. Chim. Acta*, 2004, **347**, 25–39, DOI: 10.1016/j.cccn.2004.04.023.
7 M. T. Galceran, F. J. Santos and N. H. Snow, in *Encyclopedia of Analytical Science*, 2019, pp. 148–157, DOI: 10.1016/B978-0-12-409547-2.14472-5.
8 K. Robards, in *Encyclopedia of Analytical Science: Second Edition*, 2004, pp. 1–7. DOI: 10.1016/B0-12-369397-7/00217-X.
9 R. L. Grob and E. F. Barry, *Modern Practice of Gas Chromatography*, John Wiley & Sons, Hoboken, New Jersey, 2004. DOI: 10.1002/0471651141.
10 J. J. van Deemter, F. J. Zuiderweg and A. Klinkenberg, *Chem. Eng. Sci.*, 1956, **5**, 271–289, DOI: 10.1016/0009-2509(56)80003-1.
11 M. Galletta, M. Zoccali, N. Jones, L. Mondello and P. Q. Tranchida, *Anal. Bioanal. Chem.*, 2022, **414**, 6371–6378, DOI: 10.1007/s00216-022-04086-4.
12 T. M. McGinitie, B. R. Karolat, C. Whale and J. J. Harynuk, *J. Chromatogr., A*, 2011, **1218**, 3241–3246, DOI: 10.1016/j.chroma.2010.09.068.
13 S. A. Mjøs and H. D. Waktola, *J. Sep. Sci.*, 2015, **38**, 3014–3027, DOI: 10.1002/jssc.201500364.
14 J. Ellis and K. Kounovsky-Shafer, *ACS Chem. Health Saf.*, 2023, **30**, 151–155, DOI: 10.1021/acs.chas.3c00020.
15 L. Cucinotta, E. Irrera, F. Cannizzaro, D. Sciarrone and L. Mondello, *Green Anal. Chem.*, 2025, **13**, 100255, DOI: 10.1016/j.greeac.2025.100255.
16 J. A. Muñoz-Guerra, P. Prado and S. V. García-Tenorio, *J. Chromatogr., A*, 2011, **1218**, 7365–7370, DOI: 10.1016/j.chroma.2011.08.009.
17 M. Reisch, *Chem. Eng. News*, 2017, **95**, 11–11, DOI: 10.1021/cen-09526-notw11.
18 S. Wilkinson and F. Gerth, *Reg. Sci. Environ. Econ.*, 2024, **1**, 78–103, DOI: 10.3390/rsee1010006.
19 O. Massol and O. Rifaat, *Res. Energy Econ.*, 2018, **54**, 186–211, DOI: 10.1016/j.reseneeco.2018.08.003.
20 E. Grynia and P. Griffin, *J. Nat. Gas Eng.*, 2019, **1**, 163–215, DOI: 10.7569/JNGE.2016.692506.
21 D. Butler, *Nature*, 2017, **547**, 16–16, DOI: 10.1038/547016a.
22 K. H. Kaplan, *Phys. Today*, 2007, **60**, 31–32, DOI: 10.1063/1.2754594.
23 M. Mehrpooya, N. G. Mood, H. Ansarinasab, A. S. Alsagri and M. Mehdipourrad, *Appl. Therm. Eng.*, 2019, **159**, 113787, DOI: 10.1016/j.applthermaleng.2019.113787.
24 S. T. Anderson, *Nat. Resour. Res.*, 2018, **27**, 455–477, DOI: 10.1007/s11053-017-9359-y.
25 G. Bechis, A. Arena, C. Bicchi, P. Rubiolo, M. Zoccali, C. Cagliero and L. Mondello, *J. Chromatogr., A*, 2025, **1758**, 466179, DOI: 10.1016/j.chroma.2025.466179.
26 K. Çetintürk, B. Güzel and O. Canlı, *Talanta*, 2025, **283**, 127180, DOI: 10.1016/j.talanta.2024.127180.
27 V. Cutillas, G. García-Gallego, M. Murcia-Morales, C. Ferrer and A. R. Fernández-Alba, *Anal. Methods*, 2024, **16**, 1564–1569, DOI: 10.1039/d3ay02119j.
28 C. N. Nnaji, K. C. Williams, J. M. Bishop and G. F. Verbeck, *Sci. Justice*, 2015, **55**, 162–167, DOI: 10.1016/j.scijus.2015.01.003.
29 H. Tayarani and A. Ramji, *Sustainability*, 2022, **14**, 12510, DOI: 10.3390/su141912510.
30 M. Hajjaji and C. Cristofari, *Renewable Energy*, 2024, **231**, 120982, DOI: 10.1016/j.renene.2024.120982.
31 M. Felgenhauer and T. Hamacher, *Int. J. Hydrogen Energy*, 2015, **40**, 2084–2090, DOI: 10.1016/j.ijhydene.2014.12.043.
32 N. I. Beyazit, *Int. J. Hydrogen Energy*, 2025, **99**, 836–851, DOI: 10.1016/j.ijhydene.2024.12.065.
33 T. Taylor, *LCGC North Am.*, 2023, **41**, 394, DOI: 10.56530/lcgc.na.ub5690a5.
34 K. J. Margolin Eren, H. F. Prest and A. Amirav, *J. Mass Spectrom.*, 2022, **57**, DOI: 10.1002/jms.4830.
35 EPA, U. S., *Method 8270E (SW-846): Semivolatile Organic Compounds by Gas Chromatography/Mass Spectrometry (GC/MS)*, EPA, U. S., Ed., Washington, DC, USA, 2014, https://www.epa.gov/esam/epa-method-8270e-sw-846-semi-volatile-organic-compounds-gas-chromatographymass-spectrometry-gc.

 This journal is © The Royal Society of Chemistry 2026

Open Access Article. Published on 09 December 2025. Downloaded on 1/24/2026 10:49:46 PM.
This article is licensed under a Creative Commons Attribution 3.0 Unported Licence.

36 ISO 14044:2006, *Environmental management – Life cycle assessment – Requirements and guidelines*, Geneva, Switzerland, 2006, https://www.iso.org/standard/38498.html.
37 ISO 14040:2006, *ISO 14040: Environmental Management – Life Cycle Assessment – Principles and Framework*, Geneva, Switzerland, 2006, https://www.iso.org/standard/37456.html.
38 G. Wernet, C. Bauer, B. Steubing, J. Reinhard, E. Moreno-Ruiz and B. Weidema, *Int. J. Life Cycle Assess.*, 2016, **21**, 1218–1230, DOI: 10.1007/s11367-016-1087-8.
39 Y. Xiong, S. Jiang, J. Yi and Y. Ding, *Energies*, 2024, **17**, 1530, DOI: 10.3390/en17071530.
40 U.S. Geological Survey, Helium, in *Minerals Yearbook 2022 - Metals and Minerals [Advance Release]*, 2023.
41 A. T. Jones, R. B. E. Down, C. R. Lawson, D. Keeping and O. Kirichek, *Low Temp. Phys.*, 2023, **49**, 967–970, DOI: 10.1063/10.0020164.
42 S. Evangelisti, C. Tagliaferri, D. J. L. Brett and P. Lettieri, *J. Cleaner Prod.*, 2017, **142**, 4339–4355, DOI: 10.1016/j.jclepro.2016.11.159.
43 A. Mayyas, M. Wei and G. Levis, *Int. J. Hydrogen Energy*, 2020, **45**, 16311–16325, DOI: 10.1016/j.ijhydene.2020.04.163.
44 S. Shiva Kumar and H. Lim, *Energy Rep.*, 2022, **8**, 13793–13813, DOI: 10.1016/j.egyr.2022.10.127.
45 K. Bareiß, C. de la Rua, M. Möckl and T. Hamacher, *Appl. Energy*, 2019, **237**, 862–872, DOI: 10.1016/j.apenergy.2019.01.001.
46 W. D. Seider, J. D. Seader, D. R. Lewin and S. Widagdo, *Product and Process Design Principles: Synthesis, Analysis and Design*, Wiley, 2016.
47 J. Dufour, D. P. Serrano, J. L. Gálvez, J. Moreno and C. García, *Int. J. Hydrogen Energy*, 2009, **34**, 1370–1376, DOI: 10.1016/j.ijhydene.2008.11.053.
48 S. Hellweg and L. M. I. Canals, *Science*, 2014, **344**, 1109–1113, DOI: 10.1126/science.1248361.
49 R. Elshout, *Chem. Eng.*, 2010, **117**, 34–38.
50 M. Z. Hauschild, M. Goedkoop, J. Guinée, R. Heijungs, M. Huijbregts, O. Jolliet, M. Margni, A. De Schryver, S. Humbert, A. Laurent, S. Sala and R. Pant, *Int. J. Life Cycle Assess.*, 2013, **18**, 683–697, DOI: 10.1007/s11367-012-0489-5.
51 M. A. J. Huijbregts, Z. J. N. Steinmann, P. M. F. Elshout, G. Stam, F. Verones, M. Vieira, M. Zijp, A. Hollander and R. Van Zelm, *Int. J. Life Cycle Assess.*, 2017, **22**, 138–147, DOI: 10.1007/s11367-016-1246-y.
52 M. P. Maniscalco, S. Longo, M. Cellura, G. Miccichè and M. Ferraro, *Environments*, 2024, **11**, 108, DOI: 10.3390/environments11060108.
53 F. Degen and M. Schütte, *J. Cleaner Prod.*, 2022, **330**, 129798, DOI: 10.1016/j.jclepro.2021.129798.
54 B. P. Weidema, M. Pizzol, J. Schmidt and G. Thoma, *J. Cleaner Prod.*, 2018, **174**, 305–314, DOI: 10.1016/j.jclepro.2017.10.340.
55 R. Turconi, A. Boldrin and T. Astrup, *Renewable Sustainable Energy Rev.*, 2013, **28**, 555–565, DOI: 10.1016/j.rser.2013.08.013.